Supplementary material for manuscript "Doublon formation by ions impacting a strongly correlated finite lattice system"

K. Balzer, M.R. Rasmussen, N. Schlünzen, J.-P. Joost, and M. Bonitz

October 22, 2018

This supplement contains additional information on 1. the Landau–Zener dimer model, 2. additional simulation results that analyze the influenc of reduced hopping rates at the edge of finite honeycomb clusters, and 3. additional simulation results for the case of long range Coulomb interaction.

1 Time-dependent Landau–Zener model for a dimer interacting with a projectile

The Landau–Zener (LZ) model [1] has been applied to doublon formation in optical lattices where the lattice depth or interaction strength were changed adiabatically [2, 3]. Here we extend the model to a different situation: the interaction of a classical projectile with a strongly correlated dimer. In this case, the external potential varies non-monotonically (see Fig. 2.a of the main text) reaching its (negative) maximum when the projectile is in the cluster plane. Therefore, a LZ transition will occur only if the system remains in the upper state after a *two-fold (forward and backward) passage of the avoided level crossing.*

As explained in the paper this problem can be solved exactly by diagonalizing the time-dependent hamiltonian. The four energy eigenvalues of the dimer, $E_0 \leq E_1 \leq E_U \leq E_2$, before the impact are well known and given by

$$\begin{aligned} E_0 &= \frac{1}{2}\left(U - \sqrt{16J^2 + U^2}\right) \\ E_1 &= 0 \\ E_U &= U \\ E_2 &= \frac{1}{2}\left(U + \sqrt{16J^2 + U^2}\right) \end{aligned}$$

Furthermore, in the presence of the potential $W(t)$ the solutions become

$$\begin{aligned} E_0(t) &= R_1(t) \\ E_1(t) &= W(t) \\ E_U(t) &= R_2(t) \\ E_2 &= \frac{1}{2}\left(U + \sqrt{16J^2 + U^2}\right) \end{aligned}$$

where R_1 and R_2 are the first and second root of the third-order polynomial equation

$$R^3 + (-2U - 3W)R^2 + (-4J^2 + U^2 + 2W^2 + 4UW)R - 2UW^2 + 4J^2U + 4J^2W - U^2W = 0\,. \tag{S1}$$

The four solutions are shown in Figure 2.a of the main text versus $W(t)$. Starting in the triplet ground state (E_0), for $t = -\infty$, the dimer undergoes a transition to the second excited state (E_U) via an avoided crossing when $W(t)$ is switched on sufficiently fast. Using a reduced two-level Landau–Zener picture, the probabilities to find the system at maximum field $W(t)$ in states E_U and E_0 can be approximated by p and $(1-p)$, respectively, where p denotes the LZ transition probability for a single diabatic passage of the crossing,

$$p = \exp\left(-\frac{2\pi V^2}{\hbar |dE/dt|}\right), \quad V = \frac{1}{2}\min_{W(t)} E\,, \tag{S2}$$

and $E = E_U - E_0$. To evaluate Eq. (S2) we use $\frac{dE}{dt} = \frac{dE}{dW}\frac{dW}{dt} = -\frac{dE}{dW}\frac{tW(t)}{\tau^2}$, set $t = \pm\tau$ [turning points of $W(t)$] and obtain

$$p = \exp\left(-\frac{2\pi\, e^{1/2}\, V^2 \tau}{\hbar W_0 |dE/dW|}\right) . \tag{S3}$$

From Fig. 2.b of the main text, we furthermore observe that V and dE/dW are almost independent of U: $2V \approx 2.826J$ and $|dE/dW| \approx 0.976$, around $W(t) = -W_0$, therefore, the probability p only depends (for fixed U) on the duration τ of the excitation.

When the projectile is leaving the dimer, the system is then transferred via another avoided level crossing from E_0 at maximum field to E_U at zero field with a conditional probability $(1-p)p$ and from E_U at maximum field to E_U at zero field with a conditional probability $p(1-p)$. The overall probability that the dimer, for $t = +\infty$, remains in state E_U after the twofold (forward and backward) passage of the avoided level crossing can therefore be approximated by:

$$P_{E_0 \to E_U} = 2p(1-p)\,, \tag{S4}$$

With insight from the dimer model, we find parameters for particularly efficient doublon formation in the 12-site cluster of Fig. 1 of the main text: (i) the optimal on-site interaction is $U^* \approx \frac{1}{2}W^*$, where $W^* = Z \cdot 10.8J$ denotes the maximum induced potential averaged over the sites A and B; thus $U^* = 5.4J$ for $Z = 1$ ($U^* = 10.8J$ for $Z = 2$), cf. the thin grey dash-dotted line in Fig. 2.b (2.c). (ii) For $U = U^*$, the velocity v_z^*, that maximizes $d_{\rm av}^{\infty}$, decreases linearly with Z. This follows from the Landau–Zener condition, $\frac{d}{d\tau}P_{E_0 \to E_U}(\tau) = 0$, which is solved by

$$(\tau^*)^{-1} = \frac{2\pi\, e^{1/2}\, V^2}{\hbar W_0 |dE/dt| \log(2)} \propto v_z^*\,. \tag{S5}$$

2 Impact of reduced hopping rates at the cluster edge

In the main text, we considered the intra-cluster hopping to be uniform and isotropic. However, it is well known that sites at the cluster edges may have a different connectivity or a specific saturation [4], leading to a modified hopping to neighboring sites. In Fig. S1, we analyze the effect of anisotropy on the doublon formation mechanism by reducing the hopping parameter between the A sites in the 12-site cluster of Fig. 1 of the main text to a value $J' < J$, according to a larger, spatial separation of the A sites compared to the distance AB. We find similar results for $d_{\rm av}^{\infty}$ as a function of the ion velocity v_z for a charge with $Z = 1$, where the doublon yield is rather low. On the other hand, for $Z = 2$, the doublon number appears even larger, as the reduction of the hopping makes the system more similar to the Hubbard dimer, where a maximum double occupation of 0.5 can be achieved by our excitation protocol as shown in Fig. 2.c, d.

3 NEGF results for Coulomb interaction. Correlation effects

In the main text, we presented in Fig. 4 results of nonequilibrium Green functions (NEGF) simulations for the asymptotic mean doublon number as a result of a sequence of excitations with Gaussian time-dependence that all occurred on one site. While this protocol is the easiest to test in an optical lattice setup, for ion stopping in a correlated finite condensed matter system the projectile-electron interaction is, of course, Coulombic. To test what is the effect of the long-range Coulomb interaction on the doublon formation scenario here we repeat the simulations using the Coulomb potential between ion and the electrons. The quantitative results depend on a large variety of parameters including the impact point (and its possilble variation) and the timing of the subsequent impacts. For better comparison with the results in the main text we retain equal time intervals between impacts and use the same impact point – in the cluster center, as in Fig. 1. The NEGF simulations used second order Born selfenergies within the generalized Kadanoff-Baym ansatz as described in Refs. [5, 6]. The high accuracy of these simulations was verified by benchmarks against DMRG results in Ref. [7]. The comparison with the results presented in Fig. 4 reveals that all trends reported in the main text remain valid also for Coulomb interaction. In fact, the long-range character of the projectile-electron interaction even enhances doublon production since the projectile interacts simultaneously with many electrons and thereby deposits more energy.

The figure also contains results of a time-dependent Hartree–Fock calculation (inset of lower figure) that exhibits completely wrong behavior as it neglects correlation effects that are of crucial importance for the present dynamics. Already the initial state (half filling) reveals the incorrect mean doublon number, $d_{\rm av}^{\rm HF}(0) = 0.25$ because, in Hartree–Fock, $d_i^{\rm HF} = \langle \hat{n}_{i\uparrow}\rangle\langle \hat{n}_{i\downarrow}\rangle$, cf. Eq. (2). Thus, $d_{\rm av}^{\rm HF}$ only follows the one-particle density which

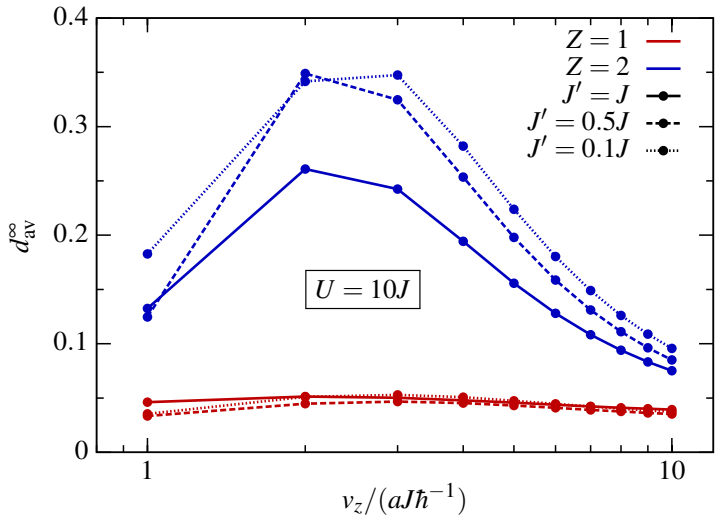

Figure S1: Ion-impact induced doublon formation in the two-dimensional Hubbard nano-cluster of Fig. 1 of the main text at $U = 10J$, where we have reduced the hopping amplitude between the A sites (along the edges of the 12-site cluster) from J to $J' = 0.5J$ (dashed) and $J' = 0.1J$ (dotted), respectively. The red (blue) lines show $d^{\infty}_{\rm av}$ as function of the projectile's velocity v_z for a positive charge of $Z = 1$ ($Z = 2$). A reduced hopping at the edges favors doublon excitation in finite clusters, in particular for high projectile charge, except for very small velocities.

exhibits a completely different time dependence than the correlated doublon number, cf. Fig. 1.a. This confirms that the present scenario, in particular, the Landau–Zener transition (see above) is a correlation effect.

References

[1] L.D. Landau, Zur Theorie der Energieübertragung. II, Phys. Z. Sowjetunion **2**, 46 (1932); G. Zener, Non-adiabatic crossing of energy levels, Proc. R. Soc. A **137**, 696 (1932).

[2] M. Schecter and A. Kamenev, Forming doublons by a quantum quench, Phys. Rev. A **85**, 043623 (2012).

[3] A.R. Kolovsky and D.N. Maksimov, Mott-insulator state of cold atoms in tilted optical lattices: Doublon dynamics and multilevel Landau-Zener tunneling, Phys. Rev. A **94**, 043630 (2016).

[4] T. Wassmann, A.P. Seitsonen, A.M. Saitta, M. Lazzeri, and F. Mauri, Structure, Stability, Edge States, and Aromaticity of Graphene Ribbons, Phys. Rev. Lett. **101**, 096402 (2008).

[5] K. Balzer and M. Bonitz, Nonequilibrium Green's Functions Approach to Inhomogeneous Systems, Lecture Notes in Physics, Springer, vol. 867 (2013).

[6] N. Schlünzen, S. Hermanns, M. Bonitz, and C. Verdozzi, Dynamics of strongly correlated fermions – ab initio results for two and three dimensions, Phys. Rev. B **93**, 035107 (2016).

[7] N. Schlünzen, J.-P. Joost, F. Heidrich-Meisner, and M. Bonitz, Nonequilibrium dynamics in the one-dimensional Fermi-Hubbard model: A comparison of the nonequilibrium Green functions approach and the density matrix renormalization group method, Phys. Rev. B **95**, 165139 (2017).

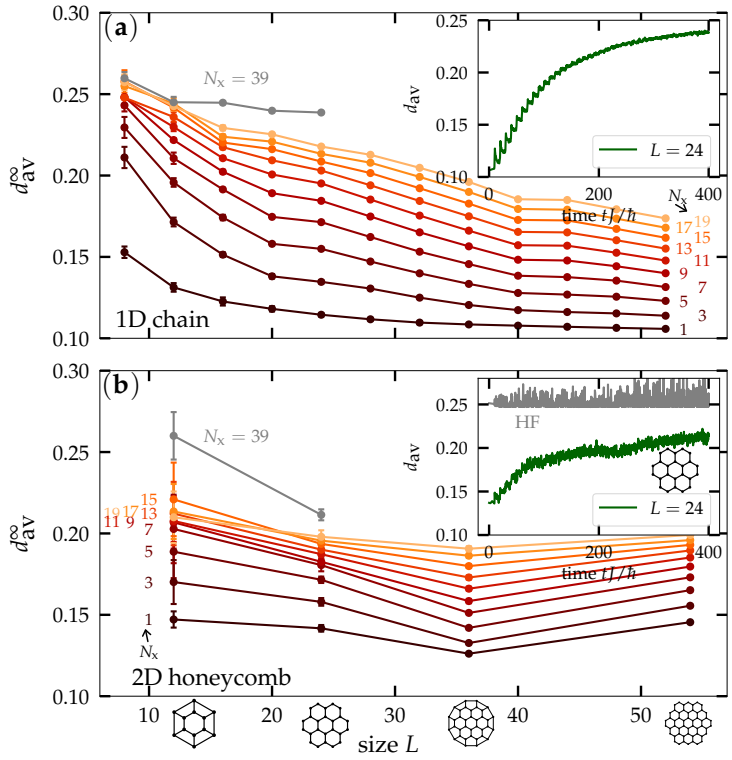

Figure S2: Asymptotic mean double occupation for a charged projectile interacting by a Coulomb potential with all electrons of the system for $U = 4J$. **a)** 1D chains and **b)** 2D half-filled honeycomb clusters of different size L. The number of excitations, N_x, which are performed in the cluster center, is indicated in the figure. All main trends are as for Gaussian-type excitation on a single site (Fig. 4), but the doublon number is enhanced. Results of NEGF simulations (second order Born selfenergies) with the HF-GKBA, for details see Refs. [5, 6]. Insets show the time-dependence $d_{av}(t)$, for $L = 24$ and $N_x = 40$. The grey curve in the lower picture corresponds to a time-dependent Hartree–Fock calculation.